Tropical Journal of Pharmaceutical Research June 2026; 25 (6): 815-822
ISSN: 1596-5996 (print); 1596-9827 (electronic)

Available online at http://www.tjpr.org
https://dx.doi.org/10.4314/tjpr.v25i6.7

Original Research Article

Synthesis, characterization, molecular docking and pharmacokinetics of new pyrimidine carboxylate derivatives as potent VEGFR inhibitors

Omeed M Hassan[1], Tiba M Hameed[2]*, Hayder B Sahib[3]
[1]Department of Pharmaceutical Chemistry, College of Pharmacy, University of Kirkuk, [2]Department of Pharmaceutical Chemistry, College of Pharmacy, [3]Department of Pharmacology and Toxicology, College of Pharmacy, Al-Nahrain University, Iraq

For correspondence:* ***Email:* *teba.majed@nahrainuniv.edu.iq;* ***Tel:*** *+9647724514664*

Sent for review: 11 May 2026 *Revised accepted: 12 June 2026*

Abstract

Purpose: *To investigate the strategic design and synthesis of three new pyrimidine carboxylate derivatives aimed at inhibiting VEGFR signaling pathways to suppress tumor growth.*
Methods: *A set of 3 new pyrimidine carboxylate derivatives was successfully synthesized via optimized chemical routes. Structural integrity of the synthesized compounds was characterized using advanced spectroscopic techniques, including FT-IR, ^{1}H-NMR, and ^{13}C-NMR. Furthermore, multidimensional in silico investigations were conducted to evaluate therapeutic potential.*
Results: *According to the simulation of molecular docking, the three derivatives demonstrated a high potential for bonding in the vascular endothelial growth factor receptor (VEGFR) active site forming stable complex structures through a series of key hydrogen bond and hydrophobic interactions between important amino acid residues. Additionally, complete ADMET profiling indicated that the three compounds have excellent pharmacokinetic profiles and high oral bioavailability.*
Conclusion: *This study shows that the synthesized pyrimidine carboxylates bind effectively with VEGFR active site, demonstrate favourable pharmacokinetic properties and high oral bioavailability.*

Keywords: *ADME, Carboxylate, Molecular docking, Pyrimidine, VEGFR*

Tropical Journal of Pharmaceutical Research is indexed by Scopus, Chemical Abstracts, Embase, Index Copernicus, EBSCO, African Index Medicus, JournalSeek, Directory of Open Access Journals (DOAJ), African Journal Online, Bioline International, Open-J-Gate and Pharmacy Abstracts

INTRODUCTION

New therapeutic strategies are undergoing development to address the growing threat of multidrug-resistant pathogens. Pyrimidine derivatives, with antitumor, antibacterial, antiviral, fungicidal, and herbicidal activity, have emerged as favourable scaffolds [1,2]. Structural modifications of pyrimidinated compounds have been shown to alter biological function [3,4]. For example, aryl-substituted 6-pyrimidin-carboxylate derivatives have been designed to replace electron-poor multi-heterocycle cores, and compounds with an ortho-carboxylate substituent at either end exhibited cytotoxic activity twice that of phenyl analogues [5-7]. *In silico* studies have been utilized for identifying candidates with cytotoxic activity against colon cancer CRC cells [8]. Computational and experimental insights into molecular recognition of potential biological targets are providing valuable guidance for structure–activity relationship studies of pyrimidine-substituted 6-carboxy compounds. Molecular docking analysis focused on top-

ranked compounds, and complexes with the highest affinity have helped researchers in identifying potential leads. Also, pharmacokinetic investigations such as absorption, distribution, metabolism, and excretion (ADME) are critical parameters in candidate selection. Therefore, this study investigated the strategic design and synthesis of three new pyrimidine carboxylate derivatives aimed at inhibiting VEGFR signaling pathways to suppress tumor growth.

EXPERIMENTAL

Preparation of the pyrimidine carboxylate

Preparation of pyrimidine carboxylate derivatives relied on a one-pot, three-component reaction of pyrimidine-2,4-dicarboxylic acid, selected aldehydes, and amines in the presence of ammonium acetate as a catalyst. All compounds were obtained in good yield, and chemical structures were elucidated by spectroscopic methods (ultraviolet-visible spectroscopy (UV–VIS), Fourier transform infrared spectroscopy (FT-IR), and nuclear magnetic resonance (NMR)). The docking studies were conducted using a validated molecular docking protocol. The binding poses of the most stable conformers were utilized for ADMET properties, cytotoxicity prediction, and metabolic analysis [9].

Chemical synthesis and characterization

The pyrimidine-5-carboxylic acid derivatives were synthesized following previously established procedures [10]. 5-Amino-2,4-dimethylpyrimidine-5-carboxylic acid was prepared via an acid-catalyzed condensation reaction between 2-amino-4-methylpyrimidine and diethyl oxalate in refluxing ethanol. The mixture was then reacted with aqueous sodium hydroxide (NaOH) and the product was obtained by a one-pot three-component reaction of pyrimidine-5-carboxylic acid, benzoylacetone, and phenyl hydrazine under ultrasonic irradiation [10]. All newly synthesized compounds were characterized using (melting point, FT-IR and NMR spectroscopy). Melting points were determined using the open capillary method.

Molecular docking protocol

Molecules library preparation

The new compounds were synthesized and characterized. Molecular docking protocols were performed for in silico analysis. The three-dimensional structure of the newly synthesized compounds was generated by Chemdraw Ultra 12.0 software [11]. After minimization of the energy. Using the semiempirical AM1 method in HyperChem 8.08 [12], we pre-optimized the structures. Following the semi-empirical optimization process mentioned above, the most stable conformation was obtained by performing a structure optimization using DFT B3LYP/6-31G [13]. The default settings indicate that the maximum force, RMS force, maximum displacement and RMS displacement have all converged to YES. The best structures were combined into a database for ligand affinity analysis with Molecular Operating Environment (MOE) software, 2019 [14].

Preparation of receptors

The crystal structure of the protein (4ASD) that was used here was acquired from Protein Data Bank database [15]. The removal of unwanted water molecules from the active site of the target protein was performed to eliminate any unnecessary hydrogen bonds that could potentially form between the ligand and the target. Once this was done, the addition of hydrogen atoms to the target protein structure was performed to create the fully protonated form of the target protein.

Ligand–protein molecular docking

The docking calculations were all done using the MOE software 2019 package. The 4ASD protein crystal structure was retrieved from the Protein Data Bank with a 2.03 Å resolution (high resolution). The docking studies were considered acceptable for 1.5 to 2.5 Å resolutions. The best RMSD should have been < 2 Å along with an energy score ≤ -7 kcal/mol; both of these metrics are traditionally used to validate results of molecular docking experiments.

Pharmacokinetic (ADME) profiling

The newly created compounds were examined for their chemical and physical properties, as well as their pharmacokinetics (absorption, distribution, metabolism, and excretion) using the Swiss ADME web server. The Swiss ADME server is used to examine the above properties [16].

RESULTS

Chemical structure of the synthesized compounds

The compounds that were synthesized included ethyl-6-methyl-2-oxo-4-phenyl-1,2,3,4-tetrahydropyrimidine-5-carboxylate (shown in

Figure 1), ethyl-4-(4-chlorophenyl)-6-methyl-2-thioxo-1,2,3,4-tetrahydropyrimidine-5-carboxylate (depicted in Figure 2), and ethyl 4-(4-chlorophenyl)-6-methyl-2-oxo-1,2,3,4-tetrahydropyrimidine-5-carboxylate (illustrated in Figure 3).

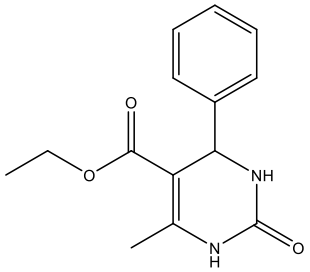

Figure 1: Ethyl-6-methyl-2-oxo-4-phenyl-1,2,3,4-tetrahydropyrimidine-5-carboxylate

FT-IR (KBr, v_max, cm−1): 3231 (N–H), 3108 (Ar–C–H), 2978 (aliphatic C–H), 1721 (C=O, ester), 1697 (C=O, amide), 1643 (C=C/C=N), 1454, 1419, 1384, 1367, 1341, 1313, 1291, 1271, 1217, 1086, 1027, 954, 878, 755, 697. 1H-NMR (400 MHz, DMSO-d_6, δ (ppm)): 9.21, s, 1H, NH; 7.75, s, 1H, NH; 7.35-7.23, m, 5H, Ar–H; 5.15, d, 1H, CH; 4.01-3.96, m, 2H, OCH2; 2.25, s, 3H, CH3; 1.11-1.06, t, 3H, CH3.^{13}C-NMR (100 MHz, DMSO-d_6, δ ppm): 165.81 (C=O, ester), 152.61 (C=O, pyrimidinone), 148.82, 145.33, 128.86, 127.73, 126.71 (Ar-C), 99.73 (C-5), 59.66 (OCH_2), 54.42 (CH), 18.25 (CH_3), 14.54 (CH_3 of ethyl).

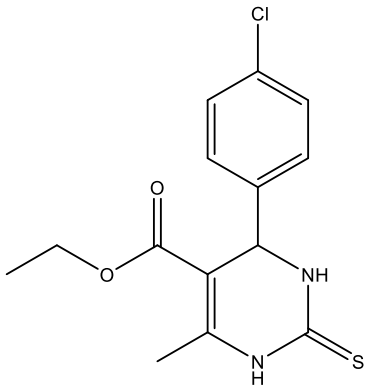

Figure 2: Ethyl-4-(4-chlorophenyl)-6-methyl-2-thioxo-1,2,3,4-tetrahydropyrimidine-5- carboxylate

FT-IR (KBr, v_max, cm^{-1}): 3323, 3170 (N–H), 3101 (Ar–C–H), 2984 (aliphatic C–H), 1669 (C=O), 1572 (C=N/C=C), 1488, 1463, 1391, 1370, 1334, 1296, 1281, 1251, 1195, 1176, 1116, 1092, 1030, 1014, 958, 874, 849, 819, 804, 744, 689, 645, 595, 558, 503, 492, 463 cm^{-1}.

^{1}H-NMR (400 MHz, DMSO-d_6, δ ppm): 10.41 (s, 1H, NH), 9.69 (s, 1H, NH), 7.95–7.91 (d, 2H, Ar–H), 7.56–7.40 (d, 2H, Ar–H), 5.19 (d, 1H, CH), 4.06–3.95 (q, 2H, OCH_2), 2.14 (s, 3H, CH_3), 1.25–1.15 (t, 3H, CH_3).

^{13}C-NMR (100 MHz, DMSO-d_6, δ ppm): 192.49 (C=S), 166.93 (C=O), 165.44, 145.85, 142.85, 139.86, 138.27, 135.28, 132.75, 131.79, 131.60, 131.49, 130.09, 129.80, 129.60, 129.16, 129.03, 128.78 (Ar-C/C=N), 100.76 (C-5), 60.11 (OCH_2), 53.94 (CH), 17.66 (CH_3), 14.45 (CH_3 of ethyl).

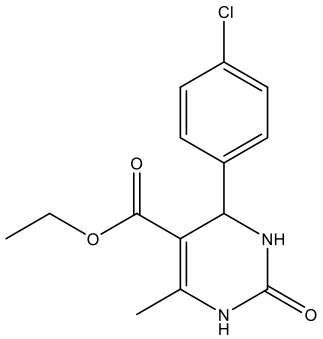

Figure 3: Ethyl 4-(4-chlorophenyl)-6-methyl-2-oxo-1,2,3,4-tetrahydropyrimidine-5-carboxylate

FT-IR (KBr, v_max, cm^{-1}): 3232 (N-H stretching), 3111 (Ar-H stretching), 2957 (Aliphatic C-H stretching), 1699 (C=O, ester), 1644 (C=O, amide), 1575 (C=C, aromatic), 1083 (C-Cl stretching).

^{1}H-NMR (400 MHz, DMSO-d_6, δ ppm): 9.27 (s, 1H, NH), 7.96–7.25 (m, 4H, Ar-H), 5.16 (d, J = 2.4 Hz, 1H, CH-pyrimidine), 4.01 (q, *J* = 6.8 Hz, 2H, OCH_2, CH_3), 2.26 (s, 3H, CH_3), 1.11 (t, *J* = 7.0 Hz, 3H, OCH_2, CH_3).

^{13}C-NMR (100 MHz, DMSO-d_6, δ ppm): 165.66 (C=O, ester), 152.45 (C=O, urea), 149.18 (C-6, pyrimidine), 144.26 (C-1', Ar), 132.27, 131.60, 128.85, 128.34 (Ar-C), 99.30 (C-5, pyrimidine), 59.72 (OCH_2), 53.91 (CH-4), 18.27 (CH_3), 14.52 (CH_3, ester).

Structural characterization of the synthesized compounds

Docking results and binding interactions

The protein binding mechanisms of the synthesized compounds (4ASD) were predicted utilizing MOE software for molecular docking analyses. Table 1 shows the predicted binding affinities and properties of the tested drugs for 4ASD. Two-dimensional and three-dimensional representations of the interaction of the

synthesized compounds with the amino acid residues of the 4ASD protein are shown in Figure 4. The results indicate the presence of hydrogen bonds and hydrophobic forces. The compounds interacted with the amino acid residues through three different mechanisms: as hydrogen donors, as hydrogen acceptors, and as hydrogen - pi interactions, as well as through two hydrogen - acceptor and pi - hydrogen interactions with water, and two pi - hydrogen interactions with the amino acid residues.

Table 1: The binding affinity and RMSD results of compounds with 4ASD

Compound	L	RMSA (Å)	Smile
1- pose1	-7.32112	1.440214	O=C(OCC)C=1{C@H}(c2ccccc2)NC(=O)NC=1C
1- pose2	-7.08691	1.046842	O=C(OCC)C=1{C@H}(c2ccccc2)NC(=O)NC=1C
1- pose 3	-6.96542	1.729081	O=C(OCC)C=1{C@H}(c2ccccc2)NC(=O)NC=1C
1- pose4	-6.90066	1.091187	O=C(OCC)C=1{C@H}(c2ccccc2)NC(=O)NC=1C
1- pose5	-6.86831	1.920697	O=C(OCC)C=1{C@H}(c2ccccc2)NC(=O)NC=1C
2- pose1	-7.25903	2.231654	Clc1ccc({C@H}2C(C(=O)OCC)=C(C)NC(=S)N2)cc1
2- pose2	-6.98458	1.559752	Clc1ccc({C@H}2C(C(=O)OCC)=C(C)NC(=S)N2)cc1
2- pose3	-6.95271	1.327868	Clc1ccc({C@H}2C(C(=O)OCC)=C(C)NC(=S)N2)cc1
2- pose4	-6.88387	0.987308	Clc1ccc({C@H}2C(C(=O)OCC)=C(C)NC(=S)N2)cc1
2- pose5	-6.83465	1.372764	Clc1ccc({C@H}2C(C(=O)OCC)=C(C)NC(=S)N2)cc1
3- pose1	-7.48642	1.889587	Clc1ccc({C@H}2C(C(=O)OCC)=C(C)NC(=O)N2)cc1
3- pose2	-7.17555	1.202615	Clc1ccc({C@H}2C(C(=O)OCC)=C(C)NC(=O)N2)cc1
3- pose3	-7.02331	1.211165	Clc1ccc({C@H}2C(C(=O)OCC)=C(C)NC(=O)N2)cc1
3- pose4	-6.99493	1.622073	Clc1ccc({C@H}2C(C(=O)OCC)=C(C)NC(=O)N2)cc1
3- pose5	-6.91154	1.046821	Clc1ccc({C@H}2C(C(=O)OCC)=C(C)NC(=O)N2)cc1
Standard (Sorafenib)	-8.11154	1.646821	Clc1c(C(F)(F)F)cc(NC(=O)Nc2ccc(Oc3cc(C(=O)NC)ncc3)cc2)cc1

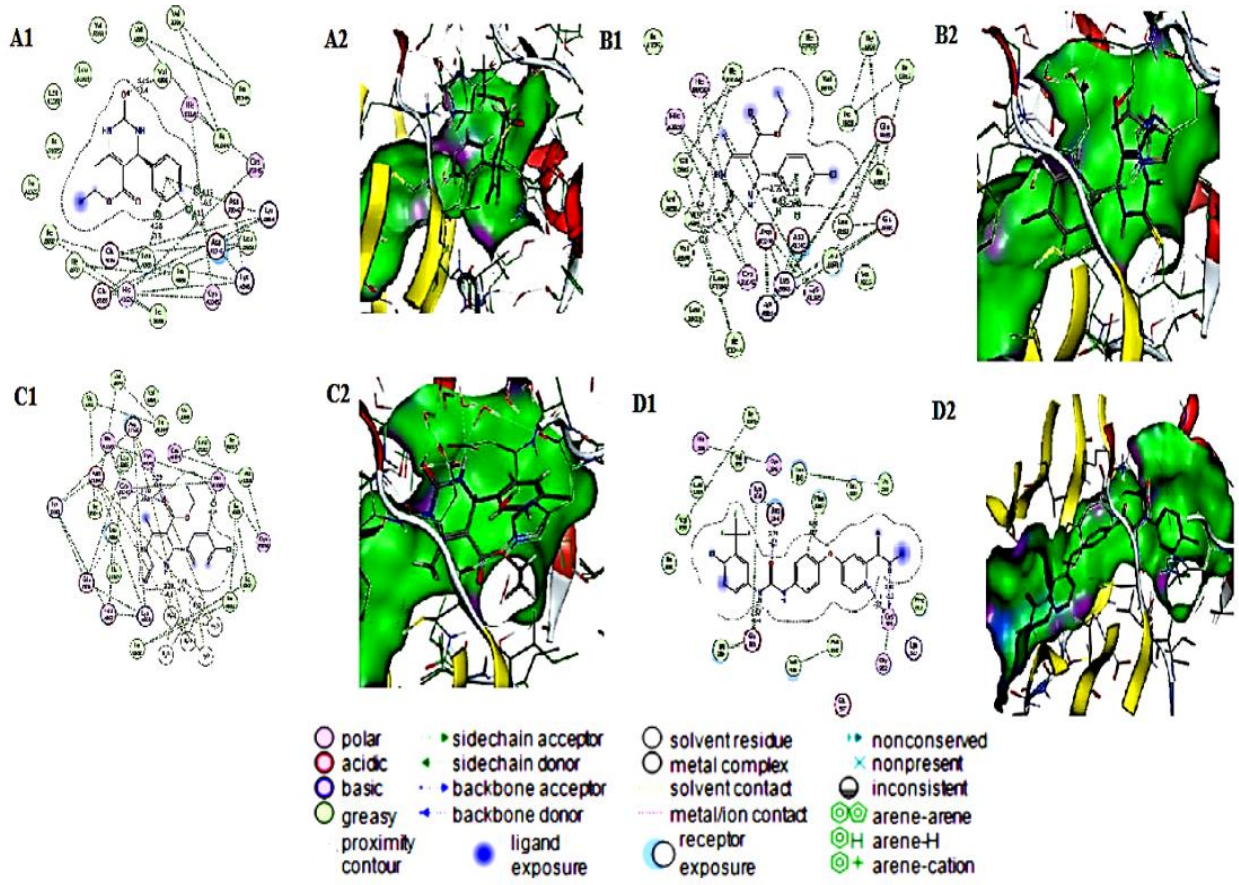

Figure 4: 2D and 3D of the best pose of the three synthesized compounds along with Sorafenib as a reference ligand. A1: 1-pose 1, B: 2-pose 2, C: 3-pose 3, D: Standard

Molecular docking results interpretations

Through a molecular docking study, we have shown that there is structural similarity between the 4ASD protein and the binding pocket formed by the ligands synthesized from our ligands by performing a systematic alignment. It is also indicated that the badging scores for some of the molecules were -6.8 to -7.5 kcal/mol when compared to the standard ligand, which has a much higher affinity of -8.11154 kcal/mol. Although all of the synthesized ligands are only moderately capable of binding to 4ASD, none of them bind as well as the standard does. Among the ligands tested, 3-pose-3 bound more effectively than the closest neighbouring ligand (-6.25199 kcal/mole), demonstrating both geometric stability (as measured by RMSD=1.889587) and multiple productive interactions (e.g., H-bonding and hydrophobic) to 4ASD through the ligand libraries created using the synthesized ligands. Compound 1-pose1 also showed favorable performance, but compound 2-pose2 had the weakest affinity (−6.98458 kcal/mol). The standard ligand (Sorafenib) established more robust interactions and stabilization, suggesting that the synthesized derivatives, though promising, require further optimization in structural and interaction capabilities to enhance receptor binding efficacy. Overall, compound 3-pose1 is the most effective synthesized ligand, targeting the 4ASD protein (Table 2).

Pharmacokinetic parameters (ADMET) Predictions

The Swiss ADME results show that all compounds generated have TPSA <140 (Table 3). Four compounds were found to satisfy Lipinski's rule of five (RO5). All the chemicals in the boiled egg were seen to have red spots in the yolk. GI passive absorption and BBB penetration of sorafenib were limited (Figure 5).

DISCUSSION

Drug design that is based on 3D structure uses computational docking to predict both the conformations and free energies of the interaction between small-molecule ligands and macromolecular targets, and is a very common method for studying biomolecular interactions and processes [17]. Molecular docking can be separated into rigid body docking and flexible body docking, with rigid body docking defining a rigid receptor and a rigid small molecule and flexible body docking defining a rigid receptor and a flexible small molecule. This type of technology has completely changed drug design research; however, it is still difficult to identify real ligands from the large pool of compound choices or to find the correct ligand conformation when binding to the target molecule. Many studies have been performed [18] while developing these techniques.

Table 2: Details of the best poses of protein 4ASD with three synthesized compounds, along with Sorafenib as a reference ligand

Compounds	Binding Affinity Kcal/mol	RMSD (Å)	Atom of compound	Atom of Receptor	Involved receptor residues	Type of interaction bond	Distance (Å)	E (kcal/mol)
1-pose1	-7.32112	1.440214	O 9	CB	VAL 898 (A)	H-acceptor	3.23	-0.4
			6-ring	CD1	LEU 889 (A)	pi-H	4.28	-0.3
			6-ring	CB	ASP 1046 (A)	pi-H	4.13	-0.6
			6-ring	CB	ASP 1046 (A)	pi-H	4.15	-0.5
2-pose2	-6.98458	1.559752	S9	CB	VAL 898 (A)	H-acceptor	3.49	-0.7
			S9	CB	VAL 898 (A)	H-acceptor	3.52	-0.6
			6-ring	N	ASP 1046 (A)	pi-H	3.75	-0.4
			6-ring	N	ASP 1046 (A)	pi-H	3.75	-0.4
3- pose1	-7.48642	1.889587	N5	O	HOH 2347 (A)	H-donor	3.29	-0.8
			N5	O	HOH 2347 (A)	H-donor	3.29	-0.6
			O19	CA	CYS 1045 (A)	H-acceptor	3.59	-0.4
			O19	CA	CYS 1045 (A)	H-acceptor	3.59	-0.4
			C15	5-ring	HIS 1026 (A)	H-pi	4.1	-0.4
Standard	-8.11154	1.646821	N3027	O	CYS 919 (A)	H-donor	2.86	-2.1
			N1240	OE2	GLU 885 (A)	H-donor	2.87	-6.4
			O1544	N	ASP 1046 (A)	H-acceptor	2.78	-2.5
			N2646	N	CYS 919 (A)	H-acceptor	3.11	-3.7
			C2015	6-ring	PHE 1047 (A)	H-pi	3.56	-0.7

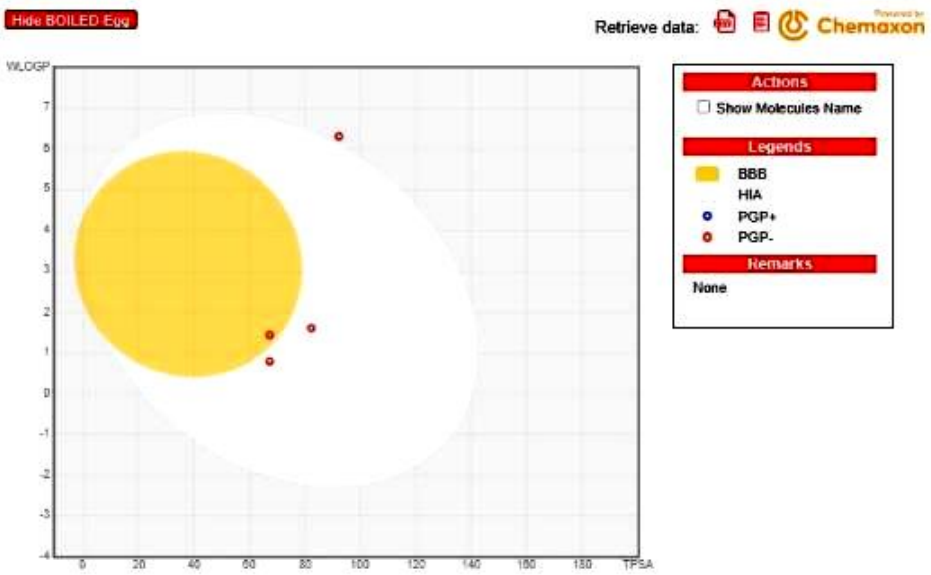

Figure 5: The BOILED-Egg representation of the synthesized compounds (1-3) along with Sorafenib

Table 3: ADME results of the synthesized compounds along with Sorafenib as a reference ligand

Compound	Molecular weight (g/moL)	H-donor	H-acceptor	MR	TPSA (Å^2)	GI-absorb	BBB permeability	Bioavailability	Lipinski's violation
SORAFENIB	464.82	3	7	112.48	92.35	low	No	0.55	0
Compound 1	260.29	2	3	77.78	67.43	High	No	0.55	0
Compound 2	310.80	2	2	89.99	82.45	High	No	0.55	0
Compound 3	294.73	2	3	82.79	67.43	High	Yes	0.55	0

Disappearance of the characteristic reactant peaks and the emergence of specific signals in FT-IR provided definitive evidence of the formation of carboxylate-functionalized pyrimidine core. The molecular docking studies demonstrated that carboxylate moiety on the pyrimidine ring enhanced binding affinity. This is primarily due to the formation of strong hydrogen bonds with key amino acids in the kinase domain of VEGFR, which mimics the binding mode of known commercial inhibitors. Orientation of the pyrimidine scaffold within the hydrophobic pocket further stabilizes the complex through pi-pi stacking interactions, suggesting a high selectivity for this receptor. Docking analysis was done to unveil inhibitory mechanisms and mode of interactions [19].

ADME properties can be determined through pharmacokinetic studies and result in the elimination of ligands from continuing development that are either unsuitable due to poor ligand properties and/or their pharmacokinetics [20]. Topological Polar Surface Area (TPSA) is an example of a property that can be used to measure a compound's ability to penetrate through biological membranes. Compounds with TPSAs less than 140 Å may exhibit good cellular permeability and bioavailability. In contrast, compounds with TPSAs > 140 Å are expected to have good bioavailability after oral administration to humans [21,22].

The Swiss ADME website provides a free resource to determine the physicochemical properties of newly created substances using in silico tools. According to pharmacokinetic reports, all twelve synthesized compounds were expected to be absorbed via passive transfer and excretion from the GI (gastrointestinal) tract to the systemic circulation, based upon their respective Topological Polar Surface Area (TOPA) values of < 140 cm^2. However, none of the synthesized compounds were expected to have the ability to traverse the Blood-Brain Barrier (BBB). Lipinski's Rule of Five (RO5) is a reliable predictive parameter used to determine drugs with usable oral bioavailability. The RO5 states that drugs with the following parameters are likely to have favorable oral bioavailability: a molecular weight < 500 dalton; no more than five hydrogen donors; no more than ten hydrogen acceptors; Log P < 5, The results of the pharmacokinetic analysis of the ten synthesized compounds indicated that the majority of the

compounds met the RO5; however, only one had an MW of > 500 [23]. The boiled egg is a tool that can be used to simply view the pharmacokinetic properties of a compound. A white area represents compounds that can cross the gastrointestinal tract by passive absorption, and a yolk area represents compounds that can cross the blood-brain barrier (BBB). Compounds represented by red dots do not get ejected from the central nervous system (CNS) through p-glycoprotein and those signified with the colour blue would be ejected by p-glycoprotein [24]. Using ADMET to profile the compounds provides a predictive analysis of the pharmacokinetic and toxicity profile of the compounds that were developed in this study. The results indicated that most derivatives are in accordance with Lipinski's RO5, which indicates good absorption from the intestines and low toxicity potential. The theoretical development illustrates the connection between chemical synthesis and biological activity. The correlation observed from the characterization of structural components with the higher binding scores that were obtained from the docking studies provides evidence that pyrimidine carboxylates are accessible through synthesis and are promising as a novel class of VEGFR inhibitors for targeted cancer therapy.

CONCLUSION

The results support the conclusion that synthesized pyrimidine carboxylates interact with the active site of VEGFR via hydrogen bonding and hydrophobic interactions, exhibit desirable pharmacokinetic properties, and are likely to demonstrate high oral bioavailability. Therefore, synthesized pyrimidine carboxylates provide excellent development candidates for the production of VEGFR-antagonists, and the data support the continuation of in vitro and in vivo biological evaluation for the use of cancer treatment.

DECLARATIONS

Acknowledgements/Funding

The authors acknowledge the contribution of the College of Pharmacy, Kirkuk University, and Al-Nahrain University, Baghdad, Iraq, in their contributions to complete this project.

Ethical Approval

Not applicable

Use of Artificial Intelligence/Language Models

The authors confirm that AI-based tools were used in a limited fashion for language editing and formatting of this manuscript (e.g., Grammar, formatting and clarity). The authors did not use AI tools to compose content, evaluate the data collected from their studies, or impact the study's design, outcome or conclusions. All original materials, data and analyses throughout the manuscript were developed and conducted by the authors.

Availability of data and materials

The datasets from this article are available upon request from the corresponding author.

Conflict of interest

There is no conflict of interest for this work.

Contribution of authors

The authors of the article declare that this work was conducted by them. The authors also declare that all liabilities relating to any claim(s) against the authors, relating to the content of this article, will be the responsibility of the author(s). We agree that OMH conceived and developed the study, TMH designed the data analysis and collected the data, and OMH wrote the manuscript. The authors stated they have all read and approved the final manuscript to be published.

REFERENCES

1. *Tiwari SV, Seijas JA, Vazquez-Tato MP, Sarkate AP, Lokwani DK, Nikalje AP. Ultrasound-mediated one-pot, three-component synthesis, docking and ADME prediction of novel 5-Amino-2-(4-chlorophenyl)-7-substituted phenyl-8,8a-dihydro-7H-(1,3,4) thiadiazolo (3,2-α) pyrimidine-6-carbonitrile derivatives as anticancer agents. Molecules 2016; 21(8): 894*
2. *Althobaiti IO, Alserhani MSM, Arafa WAA, Ghoneim AA, Hussein MF, Ibrahim HM, et al. Efficient protocol for the synthesis of novel hybrid pyrimidines: antiproliferative activity, DFT analyses, and molecular docking studies. ACS Omega 2023; 8(49): 47239-47253*
3. *Natarajan R, Anthoni Samy HN, Sivaperuman A, Subramani A. Structure-activity relationships of pyrimidine derivatives and their biological activity - A Review. Med Chem 2022; 19(1): 10-30*
4. *Keshk RM, Salama ZA, Elsaedany SK, ElRehim EM, Beltagy DM. Synthesis, antimicrobial, anti-inflammatory, antioxidant and cytotoxicity of new pyrimidine and*

pyrimidopyrimidine derivatives. Sci Rep 2025; 15(1): 9328

5. *Islam MW, Islam MM, Akter R, Limon TR, Vasquez ES, Shaikh MA, et al. A review on pyrimidine-based derivatives: synthesis and their biological application. J Heterocycl Chem 2024; 61(7): 1159-1179*
6. *Elumalai K, Shanmugam A, Devaraji M, Srinivasan S. Synthesis and molecular docking of pyrimidine derivatives as antibacterial agents. Carbon Resour Convers 2024; 7(3): 100222*
7. *Hassaballah AI, El-Ziaty AK, Ewies EF, Zayed EM, Mohamed GG. Synthesis of pyrimidine ligand and its mononuclear metal (II)/(III) complexes: Spectroscopic characterization, thermal, DFT, molecular docking, antimicrobial and anticancer studies. Inorg Chem Commun 2023; 155: 110989*
8. *Hamid IK, Attia KAA. Synthesis, characterization and evaluation of the bacterial, antioxidant and anticancer activity of pyrimidine derivatives. Int J Health Sci 2022; 6(S1): 14542–14559*
9. *Hameed TM, Abdulqader KA, Abdulnabi AA, Alawad KM, Hamid AA. Docking, dynamic simulation and ADME studies of new 1, 2, 3-triazole–based molecules for potential anticancer applications. Trop J Pharm Res 2026; 25(3): 315-328*
10. *Elmorsy MR, Mahmoud ES, Fadda AA, Abdel-Latif E, Abdelmoaz MA. Synthesis, biological evaluation and molecular docking of new triphenylamine-linked pyridine, thiazole and pyrazole analogues as anticancer agents. BMC Chem 2022; 16: 88*
11. *ChemDraw Ultra, CambridgeSoft Corporation, Version 12.0 (2010). Available at: https://perkinelmerinformatics.com/products/research/chemdraw*
12. *HyperChem Professional, Hypercube, Inc., Version 8.0.8 (2009). Available at http://www.hyper.com*
13. *Becke AD. Density-functional thermochemistry III. The role of exact exchange. J Chem Phys 1993; 98: 5648-5652*
14. *Molecular Operating Environment (MOE), Chemical Computing Group ULC, Montreal, QC, Canada (2019). Available at: https://www.chemcomp.com*
15. *Sastry GM, Adzhigirey M, Day T, Annabhimoju R, Sherman W. Protein and ligand preparation: parameters, protocols, and influence on virtual screening enrichments. J Comput Aided Mol Des 2013; 27(3): 221-234*
16. *Bouzabata A, Ashour ML, Bouzabata L, Elsharkawy ER, Guebli A, Grabsia A, et al. FactoMineR-based multivariate analysis and SwissADME profiling of medicinal plants against cutaneous leishmaniasis. Futur J Pharm Sci 2025; 11(1): 1-15*
17. *Forli S, Huey R, Pique ME, Sanner MF, Goodsell DS, Olson AJ. Computational protein-ligand docking and virtual drug screening with the AutoDock suite. Nat Protoc 2016; 11(5): 905-919*
18. *Torres PHM, Sodero ACR, Jofily P, Silva-Jr FP. Key topics in molecular docking for drug design. Int J Mol Sci 2019; 20(18): 4574*
19. *Emran TB, Rahman MA, Uddin MM, Dash R, Hossen MF, Mohiuddin M, et al. Molecular docking and inhibition studies on the interactions of Bacopa monnieri's potent phytochemicals against pathogenic Staphylococcus aureus. DARU 2015; 23(1): 26*
20. *Daina A, Michielin O, Zoete V. SwissADME: a free web tool to evaluate pharmacokinetics, drug-likeness and medicinal chemistry friendliness of small molecules. Sci Rep 2017; 7(1): 42717*
21. *Adnan AM, Mahdi MF, Kareem KA. Design, synthesis, and acute anti-inflammatory assessment of new 2-methyl benzoimidazole derivatives having 4-thiazolidinone nucleus. Al-Mustansiriyah J Pharm Sci 2019; 19(4): 151-160*
22. *Pajouhesh H, Lenz GR. Medicinal chemical properties of successful central nervous system drugs. NeuroRx 2005; 2(4): 541-553*
23. *Sardar MS, Iqbal MS, Hassan MM, Bu C, Hussain S. Improved QSAR methods for predicting drug properties utilizing topological indices and machine learning models. Eur Phys J 2025; 48(4): 25*
24. *Sharma G, Sahaya SB, Srivastava H, Moin S. Molecular docking and ADME analysis of the novel compound ((Z)-1a, 5-dimethyl-9-methylene-8-oxo1a, 2, 3, 6, 6a, 8, 9, 9a, 10, 10a-decahydro-11-oxa bicyclo (8.1. 0) undeca-1 (10), 4-dieno (7, 8-b) furan-10-yl acetate) isolated from Tanacetum dolicophyllum (Kitam.) Kitam. J Appl Natl Sci 2025; 17(2): 793.*